PHYSICAL REVIEW E **80**, 050601(R) (2009)

Size-dependent nucleation kinetics at nonplanar nanowire growth interfaces

T. Haxhimali,[1,2] D. Buta,[2] M. Asta,[2,*] P. W. Voorhees,[1] and J. J. Hoyt[3]
[1]*Department of Materials Science and Engineering, Northwestern University, Evanston, Illinois 60208, USA*
[2]*Department of Chemical Engineering and Materials Science, University of California, Davis, California 95616, USA*
[3]*Department of Materials Science and Engineering, McMaster University, Hamilton, Ontario L8S 4L8, Canada*
(Received 2 March 2009; published 23 November 2009)

In nanowire growth, kinetic processes at the growth interface can play an important role in governing wire compositions, morphologies, and growth rates. Molecular-dynamics simulations have been undertaken to probe such processes in a system featuring a solid-liquid interface shape characterized by a facet bounded by rough orientations. Simulated growth rates display a dependence on nanowire diameter consistent with a size-dependent barrier for facet nucleation. A theory for the interface mobility is developed, establishing a source for size-dependent growth rates that is an intrinsic feature of systems possessing growth interfaces with faceted and rough orientations.

DOI: 10.1103/PhysRevE.80.050601 PACS number(s): 81.10.Aj, 62.23.Hj, 61.46.−w, 81.07.−b

The vapor-liquid-solid (VLS) method [1] has found widespread use in the synthesis of elemental, compound, and multilayer nanowires for a wide variety of potential technological applications [2]. Due to the pronounced interest in this technique, substantial efforts have been aimed at developing theoretical models for VLS growth (e.g., [3–10]). Among the outstanding questions, an issue of primary importance concerns the nature of intrinsic size effects underlying diameter dependencies of nanowire growth rates and morphologies. Size effects in VLS growth are known to reflect the nature of the rate-limiting processes operating under given synthesis conditions [6]. For situations where the rate-limiting process is adsorption and chemical dissociation of vapor-phase molecules at the catalyst-vapor surface, growth rates have been shown to be independent of the nanowire diameter [3]. By contrast, if the rate-limiting step involves mass transport along the nanowire-vapor surface, an increasing growth rate with decreasing diameter is predicted [6,11–13]. The opposite trend is expected when the rate-limiting step is the nucleation and spreading of two-dimensional islands at the catalyst-nanowire interface. In this case size effects arise due to the transition from mononuclear to polynuclear island growth with increasing diameter [4], and the dependencies of both island nucleation and spreading rates on the system size [9,14].

It has long been appreciated that intrinsic size dependencies for island nucleation kinetics can arise through capillarity-related Gibbs-Thomson effects [14]. In VLS growth these effects are traditionally associated with the curved nanowire solid-vapor and catalyst liquid-vapor surfaces [14,15]—nanowire-catalyst interfaces are often assumed to be faceted and flat, and thus they generally have not been considered as a source of such effects. Very recently, however, experimental observations [16,17] have shown that, in some cases, in both VLS and the related vapor-solid-solid [18] growth method, the nanowire-catalyst interface can be nonplanar. In this Rapid Communication we present results of molecular-dynamics (MD) simulations demonstrating that the presence of nonplanar nanowire-catalyst interfaces with a faceted segment bounded by rough orientations gives rise to a qualitatively distinct size effect in nanowire growth. This effect is associated with a pronounced size dependence of the barrier to nucleate a new terrace at the faceted solid-liquid interface. Based on the insights from MD we develop a theory for the interface mobility, establishing that the observed size effects should be relevant at experimentally accessible crystallization velocities.

To investigate kinetic processes underlying crystallization during nanowire growth by MD, we consider the Stillinger-Weber model of elemental Si [21]. This system is known to crystallize in the diamond-cubic crystal structure and features faceted solid-liquid interfaces. By studying an elemental system, rather than the metal-catalyst/semiconductor-crystal systems typical of VLS growth, our aim is to elucidate effects associated purely with interface kinetic processes on a time scale accessible by MD simulations. The generalization of the MD results for the alloy case at experimentally relevant small driving forces is discussed in the latter part of this Rapid Communication.

In the MD simulations [19], bulk solid and liquid samples were equilibrated separately and then joined together to yield coexisting phases separated by crystal-melt interfaces oriented normal to the [111] crystallographic direction, following the procedure described in Ref. [20]. Equilibration runs were then conducted with periodic boundary conditions imposed in each of the three orthogonal directions. Subsequently, the periodic boundaries were removed in one of the directions parallel to the interface as well as in the direction perpendicular to it, producing solid-vacuum and liquid-vacuum surfaces, meeting the solid-liquid interface at a three-phase contact line. The system is then allowed to relax in constant-energy MD simulations. An example of a resulting structure is shown in Fig. 1.

An important feature of the structure in Fig. 1 is the nonplanar nature of the crystal-melt interface, which contains a (111) facet in the middle, bounded by curved regions that join smoothly to the solid-vapor and liquid-vapor surfaces at the contact line. In separate simulations for solid nanocrystals equilibrated in a bulk liquid, an equilibrium shape is

*Current address: Department of Materials Science and Engineering, University of California, Berkeley, California 94720.

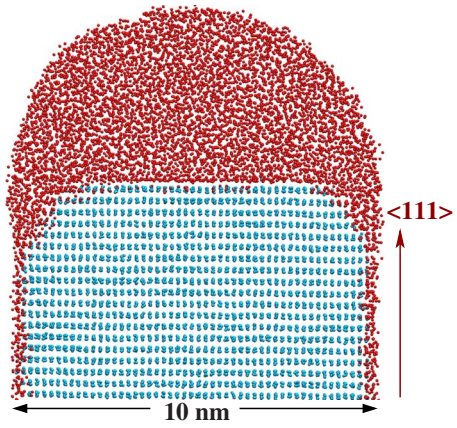

FIG. 1. (Color online) A snapshot of an equilibrated elemental nanowire. The crystal-melt interface is nonplanar with a flat faceted segment in the middle bounded by rough parts near the contact line where the three phases meet. Atoms are given different colors (red for liquid and blue for solid online) based on the value of a local structural order parameter discussed in the text. Note that the MD simulations that produced this structure employed periodic boundary conditions in the direction into the page, so that the solid-liquid interface has the shape shown in the plan views of Fig. 2.

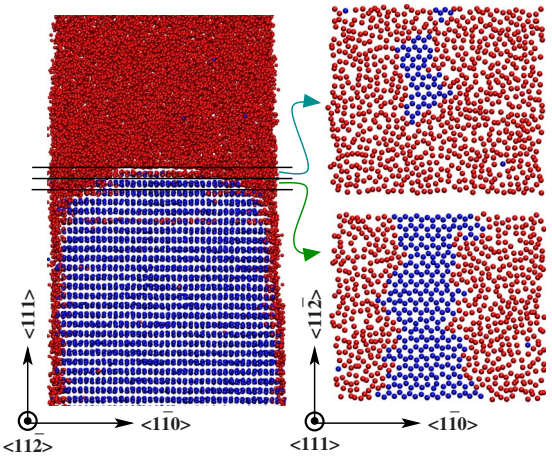

FIG. 2. (Color online) A cross-sectional view of the solid-liquid interface in a growing 7.7 nm nanowire is shown on the left. The figures on the right are plan views of the layers on top of and below the growing interface. The presence of a small crystal nucleus on the top right panel is apparent, located on the underlying crystal terrace shown below. Note that the simulation cell shown on the left is periodic in the direction into the page.

obtained that also features {111} facets bounded by curved rough orientations; the interface shown in Fig. 1 is thus interpreted to represent a portion of the equilibrium Wulff shape. Qualitatively, the nonplanar geometry of the solid-liquid interface in Fig. 1 is similar to the nanowire-catalyst interfaces observed by Sutter and Sutter [16] for Ge VLS nanowires at 748 K.

To study the kinetics of the solid-liquid interface a driving force for crystallization is provided by cooling the system below its (size-dependent) coexistence temperature. For the geometries illustrated by Fig. 1 it proved difficult to achieve steady-state growth. For the results discussed in the remainder of this Rapid Communication, we found it to be advantageous to retain the periodic boundary conditions along the growth direction during the equilibration and subsequent growth simulations. This implies the presence of two solid-liquid interfaces within the simulation cell. The left panel of Fig. 2 illustrates the geometry of the simulation cell, zoomed in to highlight the structure of one of the solid-liquid interfaces. The interface shape and contact line are seen to be similar to that shown in Fig. 1—differences in facet width and interface roughness are due to shape fluctuations and terrace nucleation, which are more pronounced for the smaller size and growth conditions associated with Fig. 2 [22].

To study the effect of the nanowire size on the interface kinetics we prepared three samples with widths $D=5$, 7.7, and 10 nm. After equilibrating each, the final coexistence temperatures (T_c) were found to be size dependent; values of $T_c=1589$, 1625, and 1637 K, were obtained for $D=5$, 7.7, and 10 nm, respectively, using the coexistence method described in Refs. [20,23] to obtain values of T_c to a precision of a few K. These represent undercoolings ($\Delta T_c \equiv T_M - T_c$) relative to the bulk melting temperatures ($T_M=1677$ K) of 88, 52, and 40 K, respectively, due to a Gibbs-Thomson capillarity effect associated with the curvature of the rough parts of the solid-liquid interface. For the geometry considered here the rough orientations can be approximated as having a cylindrical shape and the appropriate expression for the capillary undercooling is $\Delta T_c=(\sigma_c V_m T_M/L)/R$, where V_m is the solid atomic volume, L is the latent heat of melting (per atom), σ_c is the interfacial free energy of the rough portions of the solid-liquid interface (assumed isotropic), and $R=D/2$. The MD data for ΔT_c are well fit by this relation with $\sigma_c=0.32$ J/m^2.

Growth simulations were performed at temperatures $T=T_c-\Delta T_k$, representing finite undercoolings (ΔT_k) below T_c. In discussing the results of these simulations in the context of the theoretical model below, it will be convenient to express the thermodynamic driving force through the dimensionless variable $\beta=\Delta T_k/\Delta T_c$. Values of ΔT_k ranging between 10 and 30 K were employed in these growth simulations. Results are shown in Fig. 3, which plots the measured growth velocities (V) versus β for the three nanowire sizes. The solid lines represent best fits of the theoretical model described below. The most important aspect of the results plotted in Fig. 3 is the strong size dependence of the relationship between V and β. Specifically (see the inset), the growth velocity at a fixed driving force is seen to increase significantly with decreasing size.

To gain insight into the growth mechanisms we used an analysis employing a local structural order parameter designed to distinguish between atoms in solid and liquid phases [23]. This order parameter has been used also to color Figs. 1 and 2, where the liquid and solid atoms for which the parameter was below or above a certain threshold, respectively, are shown in different colors (red for liquid and blue for solid online). In Fig. 2 we show a snapshot of a 7.7-nm-wide nanowire during growth. The panel on the left of Fig. 2 shows a cross-sectional view of one of the two growing interfaces, and on the right are plan views of the two layers above and below the solid-liquid interface. These latter con-

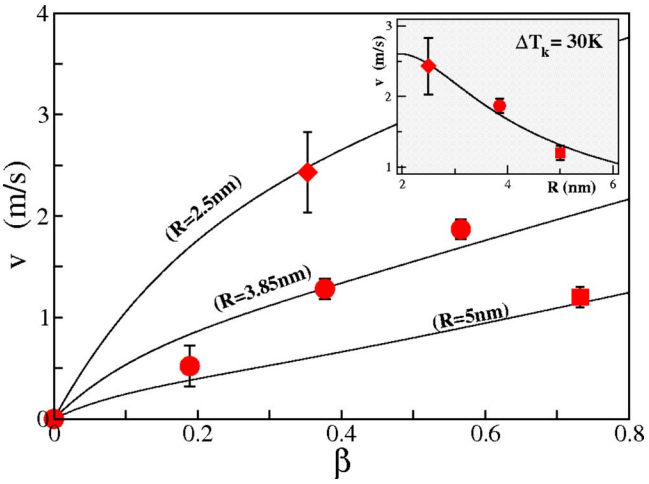

FIG. 3. (Color online) Growth velocity V versus the dimensionless driving force β. The lines represent a fit of the theoretical model described in the text to the simulation data represented by symbols for each of the system sizes studied. In the inset we plot V versus size R for a fixed ΔT_k. Error bars denote 95% error bars in the measured values of V.

tain atoms within layers of thickness $a=0.3$ nm, the distance between neighboring {111} bilayers in the Si diamond structure. The presence of a small solid nucleus located on top of the crystal terrace is apparent. From such visualizations, it is observed that the crystal grows in a layer-by-layer mode, with new crystalline layers forming through nucleation and spreading of a single nucleus. In addition to the growth simulations, we performed long MD runs under equilibrium conditions ($\beta=0$). In these simulations both facet growth (fg) and facet shrinkage (fs) processes can be observed; the former involves the formation of new layers through the terrace-nucleation mechanism, while the latter occurs by melting inward from the periphery. Based on the insights derived from the MD simulations and models for the dynamics of faceted interfaces in pure materials [24–28], we develop the following kinetic theory for nanowire growth, applicable to both pure systems (with thermally driven growth, as in the MD simulations) and alloys (with growth driven by supersaturation, as in experiment) with growth interfaces containing a facet bounded by rough orientations.

We consider the interface geometry illustrated in Fig. 4, for which the net nanowire growth velocity reflects a balance between the fg and fs processes: $V=V_{fg}-V_{fs}$. Facet growth and shrinkage are assumed to have activated rates: $V_{fg}=V_0\exp(-\varepsilon^*_{fg}/k_BT)$ and $V_{fs}=V_0\exp(-\varepsilon^*_{fs}/k_BT)$, where ε^*_{fg} and ε^*_{fs} are nucleation barriers and V_0 is a kinetic prefactor. To derive expressions for the nucleation barriers we model the nanowire geometry as in Fig. 4. The facet has a radius (ρ) expressed as $\rho=R\sin(\theta)$, in terms of the nanowire radius R and the angle θ between the rough and faceted parts of the solid-liquid interface. In three dimensions, we assume that the rough portions of the solid-liquid interface have the shape of a truncated sphere capped by a circular facet. In this geometry, the free energy to form a circular nucleus can be written as $\varepsilon=2\pi r\gamma-\pi r^2 a\Delta\Omega$. Here, γ denotes the energy of the step at the periphery of the cluster, which can be related

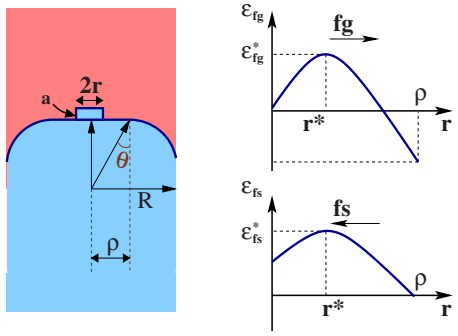

FIG. 4. (Color online) A schematic representation of a crystal nucleus on the faceted terrace is shown in the left figure, which also defines the variables introduced in the theoretical model described in the text. The energies to grow crystal nuclei and to shrink an underlying terrace are plotted schematically on the right.

to the interfacial free energy (σ_c) through the relation $\gamma=a\sigma_c\sin(\theta)$ [24]. $\Delta\Omega$ is the difference in the grand potential (per volume) between liquid and solid phases, which contains two contributions, associated with the capillary driving force ($\Delta\Omega_c=2\sigma_c/R$) and the kinetic undercooling ($\Delta\Omega_k$). As above, we define $\beta=\Delta\Omega_k/\Delta\Omega_c$.

The net result is an energy to form a nucleus through fg or fs mechanisms illustrated on the right of Fig. 4. It can be shown (see supplemental material [29]) that

$$r^* = \rho/2(1+\beta),$$

$$\varepsilon^*_{fg} = \varepsilon^*_0/(1+\beta),$$

$$\varepsilon^*_{fs} = \varepsilon^*_0(1+2\beta)^2/(1+\beta). \quad (1)$$

The equilibrium nucleation barrier ε^*_0 is given by the size-dependent relation,

$$\varepsilon^*_0 = \pi R a\sigma_c \sin^2(\theta)/2. \quad (2)$$

For elemental systems with $\beta=0$, Eqs. (1) and (2) reduce to the formulas for terrace nucleation on faceted nanoparticles derived by Mullins and Rohrer [24]. The final expression for the growth velocity is

$$V(\beta) = V_0[\exp(-\varepsilon^*_{fg}/k_BT) - \exp(-\varepsilon^*_{fs}/k_BT)]. \quad (3)$$

To check the validity of this theory we compare its predictions with the MD results. For the pure system and quasi-two-dimensional geometry considered by MD, it can be shown that the above theoretical model predicts the same form for the dependence of V on β as given by Eqs. (1) and (3). In the MD case, $\beta=\Delta T_k/\Delta T_c$ and ϵ^*_0 is given by multiplying Eq. (2) by a geometrical factor of $2/\pi$. Inserting these expressions into Eq. (3) leads to a model that can be fit to the MD data. In this fit, we make use of the value of $\sigma_c=0.32$ J/m^2 (see above). There remain two fitting parameters: $\sin(\theta)$ and V_0. The fit is shown in Fig. 3, where the optimal parameter values are $\sin(\theta)=0.45(5)$ and $V_0=12(4)$ m/s. The value of $\sin(\theta)$ is reasonable, as it implies an equilibrium facet radius that is roughly half the nanowire diameter, which is consistent with the images in Figs. 1 and 2. As shown in the inset to Fig. 3, the model accurately

describes the size dependence of the MD growth velocities.

The MD results establish a significant size effect on facet nucleation kinetics for nanowire growth in a pure system. It remains to establish that the effect is relevant to nanowires grown from alloy catalysts at realistic growth rates that are orders of magnitude lower than those characteristic of the MD simulations. The very small interface velocities found in nanowire growth experiments implies small driving forces, i.e., $\beta \ll 1$ in Eqs. (1) and (3). In the supplemental material [29] it is shown that in this limit Eq. (3) for the interface velocity V can be written in the form $V(R,\Delta C)=M(R)\Delta C$, where $M(R)$ is a size-dependent interface mobility given as

$$M(R) = V_0\left(\frac{R}{d_1}\right)^2 \exp\left(\frac{-R}{d_2}\right). \tag{4}$$

Here, $d_1=\sqrt{V_m^w k_B T/\pi G'' a \sin^2(\theta)(1-C^{le})}$ and $d_2=2k_BT/\pi a \sigma_c \sin^2(\theta)$, where G'' is the second derivative of the catalyst molar free energy with respect to solute concentration, evaluated at the equilibrium solute concentration C^{le}, and V_m^w is the molar free energy of the nanowire. The magnitudes of d_1 and d_2 can be estimated with the parameters given above to be on the order of nanometers for typical growth temperatures. Equation (4) predicts that the mobility reaches a maximum at $R=2d_2$, beyond which $M(R)$ decreases strongly with increasing nanowire size, as observed in MD. The analysis thus establishes that the dependence of the nanowire-catalyst interface velocity on the wire radius found in the MD simulations is expected to hold also for alloy catalysts and experimentally relevant growth rates. It is thus expected that the size effect elucidated in this work is an intrinsic feature of crystal growth in systems that display interfaces with both faceted and rough orientations.

This research was supported by the National Science Foundation Grant No. CMMI-0507053 (T.H., P.W.V., and M.A.) and the U.S. Department of Energy, Office of Basic Energy Sciences Grant No. DE-G02-06ER46282 (D.B. and J.J.H.). We acknowledge helpful discussions with Alain Karma.

[1] R. S. Wagner and W. C. Ellis, Appl. Phys. Lett. **4**, 89 (1964); R. S. Wagner, in *Whisker Technology*, edited by A. P. Levitt (Wiley, New York, 1970).

[2] K. Haraguchi, T. Katsuyama, K. Hiruma, and K. Ogawa, Appl. Phys. Lett. **60**, 745 (1992); F. Patolsky *et al.*, Proc. Natl. Acad. Sci. U.S.A. **101**, 14017 (2004); C. Thelander *et al.*, Appl. Phys. Lett. **83**, 2052 (2003).

[3] S. Kodambaka, J. Tersoff, M. C. Reuter, and F. M. Ross, Phys. Rev. Lett. **96**, 096105 (2006).

[4] D. Kashchiev, Cryst. Growth Des. **6**, 1154 (2006).

[5] L. E. Fröberg, W. Seifert, and J. Johansson, Phys. Rev. B **76**, 153401 (2007).

[6] V. G. Dubrovskii, N. V. Sibirev, G. E. Cirlin, J. C. Harmand, and V. M. Ustinov, Phys. Rev. E **73**, 021603 (2006); V. G. Dubrovskii and N. V. Sibirev, J. Cryst. Growth **304**, 504 (2007).

[7] V. Schmidt, S. Senz, and U. Gösele, Phys. Rev. B **75**, 045335 (2007).

[8] S. Roper *et al.*, J. Appl. Phys. **102**, 034304 (2007).

[9] A. A. Golovin, S. H. Davis, and P. W. Voorhees, J. Appl. Phys. **104**, 074301 (2008).

[10] K. W. Schwarz and J. Tersoff, Phys. Rev. Lett. **102**, 206101 (2009).

[11] W. Dittmar and K. Neumann, in *Growth and Perfection of Crystals*, edited by R. H. Doremus, B. W. Roberts, and D. Turnbull (Wiley, New York, 1958).

[12] V. Ruth and J. P. Hirth, J. Chem. Phys. **41**, 3139 (1964).

[13] J. M. Blakely and K. A. Jackson, J. Chem. Phys. **37**, 428 (1962).

[14] E. I. Givargizov and A. A. Chernov, Kristallografiya **18**, 147 (1973); Sov. Phys. Crystallogr. **18**, 89 (1973); E. I. Givargizov, J. Cryst. Growth **31**, 20 (1975).

[15] E. J. Schwalbach and P. W. Voorhees, Nano Lett. **8**, 3739 (2008).

[16] E. Sutter and P. Sutter, Nano Lett. **8**, 411 (2008).

[17] J. Drucker (private communication).

[18] A. I. Persson *et al.*, Nature Mater. **3**, 677 (2004); S. Kodambaka, J. Tersoff, M. C. Reuter, and F. M. Ross, Science **316**, 729 (2007).

[19] All MD simulations made use of the LAMMPS code described by S. J. Plimpton, J. Comput. Phys. **117**, 1 (1995); http://lammps.sandia.gov/index.html

[20] S. Yoo, X. C. Zeng, and J. R. Morris, J. Chem. Phys. **120**, 1654 (2004).

[21] F. H. Stillinger and T. A. Weber, Phys. Rev. B **31**, 5262 (1985).

[22] Tests were performed to establish that the periodic length parallel to the solid-liquid interface was large enough not to affect the growth rates or associated mechanisms.

[23] D. Buta, M. Asta, and J. J. Hoyt, Phys. Rev. E **78**, 031605 (2008); J. Chem. Phys. **127**, 074703 (2007).

[24] W. W. Mullins and G. S. Rohrer, J. Am. Ceram. Soc. **83**, 214 (2000); G. S. Rohrer, C. L. Rohrer, and W. W. Mullins, *ibid.* **84**, 2099 (2001).

[25] N. Combe, P. Jensen, and A. Pimpinelli, Phys. Rev. Lett. **85**, 110 (2000).

[26] M. Degawa, F. Szalma, and E. D. Williams, Surf. Sci. **583**, 126 (2005).

[27] P. Nozières, in *Shape and Growth of Crystals*, edited by C. Godrèche, Solids Far from Equilibrium (Cambridge University Press, Cambridge, England, 1991), pp. 1–154.

[28] P. Wolf, F. Gallet, S. Balibar, E. Rolley, and P. Nozières, J. Phys. (Paris) **46**, 1987 (1985).

[29] See EPAPS Document No. E-PLEEE8-80-R06911 for details of the derivation of the growth model for alloys. For more information on EPAPS, see http://www.aip.org/pubservs/epaps.html